Proceedings of the XI DINAME, 28th February-4th March, 2005 - Ouro Preto - MG - Brazil
Edited by D.A. Rade and V. Steffen Jr.

ADAPTIVE TECHNIQUES APPLIED TO OFFSHORE DYNAMIC POSITIONING SYSTEMS

Eduardo Aoun Tannuri
Department of Naval Architecture and Oceanic Engineering
University of São Paulo
eduat@usp.br

Leonardo Kenji Kubota
Department of Naval Architecture and Oceanic Engineering
University of São Paulo
leonardo.kubota@poli.usp.br

Celso Pupo Pesce
Department of Mechanical Engineering
University of São Paulo
Av. Prof. Mello Moraes, 2231, CEP 05508-900, Cidade Universitária, São Paulo, Brazil.
ceppesce@usp.br

Abstract. *Dynamic positioning systems (DPS) comprise the utilization of active propulsion to maintain the position and heading of a vessel. Several sensors are used to measure the actual position of the floating body, and a control algorithm is responsible for the calculation of forces to be applied to each propeller, in order to counteract all environmental forces, including wind, waves and current loads. The controller cannot directly compensate motions in the sea waves frequency range, since they would require an enormous power to be attenuated, possibly causing damage to the propeller system. A filtering algorithm is then used to separate high frequency components from the low frequency ones, which are indeed controlled. Usual commercial systems apply Kalman filtering technique to perform such task, due to the smaller phase lag introduced in the control loop compared to conventional low-pass filters. The Kalman filter uses a model of the system, which depends on an unknown parameter, related to wave frequency. Adaptive filtering is then applied, in order to perform an on-line estimation of such parameter. However, the control algorithms are normally based on constant gains, and performance degradation may be encountered in some situations, as those related to mass variation during a loading operation. This paper presents the application of model-based adaptive control techniques to DPS's, cascaded with the commonly used adaptive Kalman filter. The model of a dynamic positioned shuttle tanker subjected to waves and current is used to show the advantages of the adaptive controller compared to the common constant gain control.*

Keywords*: adaptive control, dynamic positioning system, Kalman filter*

1. Introduction

Dynamic Positioning Systems (DPS) are defined as a set of components used to keep a floating vessel on a specific position or track by the action of propellers. DPS includes position and heading measurement systems, a set of control algorithms and propellers. Several offshore operations are carried out using DPS, such as drilling, pipe-laying, offloading and diving support.

The environmental forces acting on a floating vessel are complex, and induce at least two distinct kinds of motions. Sea waves consist of a large number of oscillatory components, with several directions, amplitudes and phases. The resulting energy spectrum has a peak value between 0.3rad/s and 1.3rad/s. Waves generate large oscillatory forces and moment on the vessel, inducing high frequency motions (in the same frequency range of waves). Additionally, environmental loads include slowly varying disturbances caused by wind, current and wave drift forces, which induce low frequency oscillations and steady motions on vessels. DPS must suppress the low frequency motions, keeping the mean position of the vessel as close as possible to the desired point. However, high frequency motions are difficult to be handled by the control system, since they would require an enormous power to be attenuated, causing extra fuel consumption and increased rate of propellers wear-out, due to thruster modulation (high frequency oscillations in propellers).

Therefore, a sophisticated filtering algorithm must be included in the control loop. The purpose of the wave filter is to separate the high frequency oscillatory wave induced motion from the motion caused by slowly varying disturbances. Feedback control action must be implemented using the filtered low frequency vessel motion, enabling thruster modulation and all related problems to be avoided. Of course, the introduction of a wave filter in the control loop leads to increased phase shift (time lag) and to a lower stiffness (reaction to variations in input variables and disturbances). So, a good filter is one that keeps the modulation below tolerable limits while maintaining maximum system stiffness.

Earlier DPS used conventional Butterworth low-pass wave filters or notch filters, which could be easily implemented in analog circuits (Fossen, 1994). However, the main disadvantage of such filters is that additional phase lag is introduced, causing poor performance, increased oscillations and, sometimes, instability in closed loop response.

An alternative to conventional filtering is to apply observer based techniques, such as Kalman filtering. One of the main characteristics of Kalman filter is the use of available information regarding the dynamical behavior of the process. The vessel motion due to slow disturbances and due to wave action is modeled. The motion information (predicted by the filter model) is combined with available observations, and an optimum state estimator is then constructed. The vessel motion is regarded as the sum of two linearly independent response functions[1]. A low frequency model yields motions due to maneuvering forces and environmental forces due to wind, current and wave drift, and a high frequency model yields vessel response due to waves. The idea of separating the filter model into a low and a high frequency model was originally suggested by Balchen *et al.* (1976).

Kalman filter uses a model of the system, which depends on an unknown parameter, related to wave frequency. A biased estimation of wave spectrum peak frequency may degrade the performance of the filtering, affecting the overall behavior of the controller. Several frequency tracking algorithms have then been applied to such a problem, including variations on Recursive Prediction Error Method (RPEM) and Recursive Least Square (RLS) Estimation (Saelid *et al.*, 1983, Balchen *et al.*, 1980). These algorithms perform on-line frequency estimation and update the Kalman filter model. Such "adaptive filtering" approach has been extensively used in commercial DPS, as shown in Bray (1998) and (Kongsberg Simrad, 1999).

The control algorithm itself calculates thrust forces and moment based on low frequency motion estimates. Modern commercial systems still employ simple PD algorithms. The integral action is given by the direct compensation of environmental forces, which are also estimated by the Kalman filter, as will be shown in the next section.

The robustness and simplicity of PD controller are the main reasons for its extensive utilization. Furthermore, it satisfies the performance requirements of a great number of DP ships. The control parameter tuning procedure is normally done during the DPS installation, and sometimes requires the execution of some maneuvers in order to evaluate ship overall dynamics and maneuverability.

However, during extreme environmental conditions, the system may present loss of performance, since the PD parameters were adjusted under a calm sea state, as described in Bray (1998). Furthermore, in some offshore operations, oil is transferred from one moored FPSO[2] or platform to a DPS shuttle tanker. This operation lasts up to 24h, and the mass of the tanker may be increased by a factor of four, altering its dynamic properties. In this case, a constant gain controller is not adequate, what requires full attention of the operator, who must perform manual corrections in the positioning of the tanker, avoiding dangerous approximations.

Therefore, PD controller with constant gains is not adequate for ships that must operate under a wide "environmental window" or for ships that present significant mass variation during the operation. Such and other reasons lead the researchers to apply different control methodologies to the DPS. All initiatives present advantages compared to the constant gain PD, demonstrated by means of experiments or simulations. However, the research community was not able to convince operators and manufacturers, whose still rely on PD controller. Some examples of such novel controllers may be found in Katebi *et al.* (1997), Aarset *et al.* (1998) and Tannuri *et al.* (2001).

In the present paper, the problems associated to the PD controller are solved by means of a model-based adaptive controller. It is shown that the overall structure of the PD controller is still preserved, and the adaptive algorithm is responsible for the on-line correction of control gains. With the present solution, the authors try to address the problem, keeping the simplicity of the PD controller, which is one of the main reasons of its broad utilization.

The controller is developed and tested for only one degree of freedom of the ship, and a discussion about its generalization to the three-degree of freedom case is presented. Simulations are carried out considering a shuttle tanker similar to the vessels operating in Brazilian waters.

2. System modelling

The following dynamic model governs the low frequency horizontal motions of a vessel:

$$\begin{aligned}
&(M + M_{11})\ddot{x}_1 - (M + M_{22})\dot{x}_2\dot{x}_6 - M_{26}\dot{x}_6^{\,2} = F_{1E} + F_{1T};\\
&(M + M_{22})\ddot{x}_2 + M_{26}\ddot{x}_6 + (M + M_{11})\dot{x}_1\dot{x}_6 = F_{2E} + F_{2T};\\
&(I_Z + M_{66})\ddot{x}_6 + M_{26}\ddot{x}_2 + M_{26}\dot{x}_1\dot{x}_6 = F_{6E} + F_{6T}.
\end{aligned} \tag{1}$$

where I_z is the moment of inertia about the vertical axis; M is vessel total mass, M_{ij} are added mass matrix terms, F_{1E}, F_{2E}, F_{6E} are surge, sway and yaw environmental loads (current, wind and waves) and F_{1T}, F_{2T}, F_{6T} are forces and moment delivered by the propulsion system. The variables $\dot{x}_1$, $\dot{x}_2$ and $\dot{x}_6$ are the (midship) surge, sway and the yaw absolute velocities (Fig. 1), expressed in the reference frame of the ship.

[1] This can be justified via the multiple-scale method.

[2] Floating Production, Storage and Offloading System

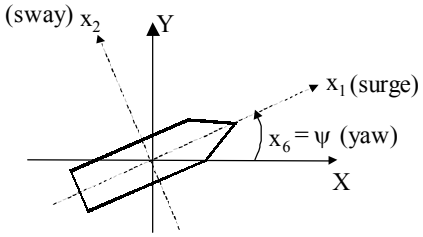

Figure 1. Coordinate systems

High frequency motions are evaluated by means of the transfer functions related to the wave height, called Response Amplitude Operators (RAOs). Such functions are obtained by numerical methods considering the potential flow around the vessel hull. This approach is based on the linear response of high frequency motions and on the uncoupling between high frequency and low frequency motions. Figure 2 shows the sway RAO for wave incidence of 90° (beam sea waves). The transfer function for a shuttle tanker (M=1.5x10^8 kg) and for a pipe-laying barge (M=0.2x10^{8}kg) are presented. As expected, the barge presents higher motions than the tanker, due to its lower inertia.

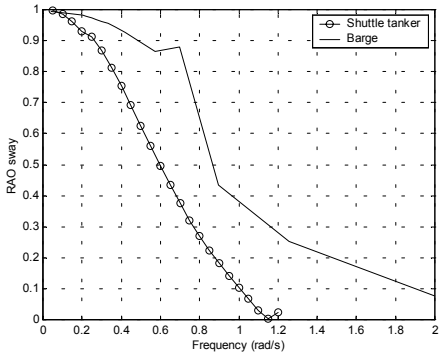

Figure 2. Sway RAO for a tanker and a barge. Beam sea wave incidence.

Real sea waves are described by a power spectrum S(ω) of surface height, and the power spectrum of ship motion *i* (P_{ii}) is then evaluated by:

$$P_{ii}(\omega) = RAO_i(\omega, \beta)^2 . S(\omega) \tag{2}$$

where β is the wave incidence angle related to the ship. The high frequency motion of the ship is then obtained by the time realization of the power spectrum function P_{ii}. Figure 3 illustrates a typical wave spectrum, for a 5.0m significant wave height and 11s peak period. Power spectra of sway motions are also presented, considering both the barge and the shuttle tanker. It should be emphasized that the peak frequency of motion spectrum may not be the same as that of the wave, due the shape of RAO function. Such fact will be addressed in the sequel.

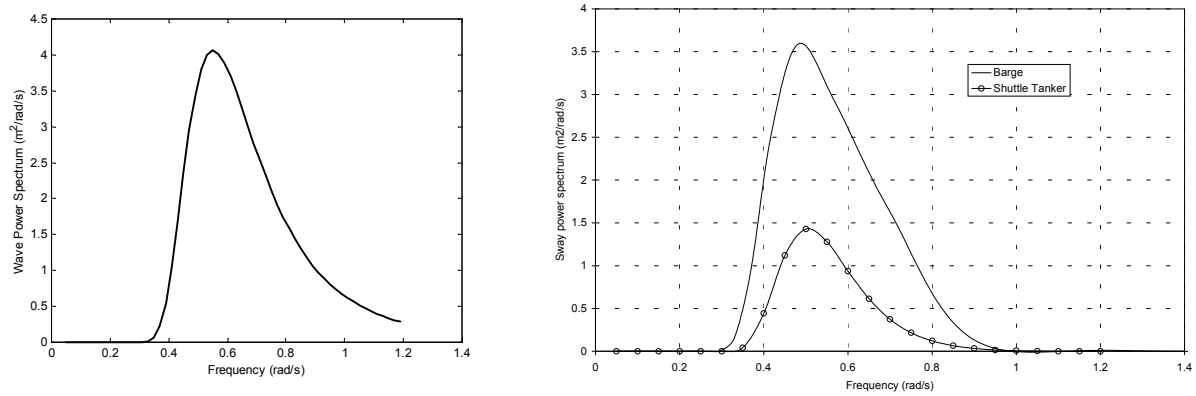

Figure 3. (Left) Wave power spectrum (5.0m wave height and 11s peak period). (Right) Spectrum of sway motion for a tanker and a barge. Beam sea wave incidence.

3. Kalman filter design

The Kalman Filter is based on simplified models for low frequency and high frequency motions of the vessel. More detailed discussions about filter design can be found in Tannuri *et al.* (2003).

Being X and Y the position of the central point of the vessel, ψ the heading angle and disregarding non-linear terms, the low frequency motion can be described by:

$$\dot{\mathbf{x}}_{\mathbf{L}} = \begin{pmatrix} \mathbf{0}_{3x3} & \mathbf{I}_{3x3} \\ \mathbf{0}_{3x3} & -\mathbf{C}_{3x3} \end{pmatrix} \mathbf{x}_{\mathbf{L}} + \begin{pmatrix} \mathbf{0}_{3x3} \\ \mathbf{M}^{-1} \end{pmatrix} \boldsymbol{\omega}_{\mathbf{L}} + \begin{pmatrix} \mathbf{0}_{3x3} \\ \mathbf{M}^{-1} \end{pmatrix} (\mathbf{F}_{\mathbf{T}} + \mathbf{F}_{\mathbf{E}}) \tag{3}$$

where $\mathbf{x}_{\mathbf{L}} = \begin{pmatrix} X_L & Y_L & \psi_L & \dot{X}_L & \dot{Y}_L & \dot{\psi}_L \end{pmatrix}^T$, $\mathbf{F_T}$ are thrusters forces and moment vector, $\mathbf{F_E}$ are low frequency environmental forces and moment vector, $\mathbf{M}$ is the mass matrix of vessel and $\mathbf{C}$ is a damping matrix. The subscript L is related to low frequency motion. In this model, it is assumed that the heading angle is less than 20^o, approximately, during the motion. $\boldsymbol{\omega}_{\mathbf{L}}$ is a 3x1 vector containing zero-mean Gaussian white noises processes with covariance matrix $\mathbf{Q_L}$ ($\boldsymbol{\omega}_{\mathbf{L}} \sim N(0, \mathbf{Q}_{\mathbf{L}})$)

The forces $\mathbf{F_E}$ are slowly varying unknown variables, and can be modeled by:

$$\dot{\mathbf{F}}_{\mathbf{E}} = \boldsymbol{\omega}_{FL} \tag{4}$$

where $\omega_{\mathbf{FL}}$ is a 3x1 vector containing zero-mean Gaussian white noises processes with covariance matrix $\mathbf{Q_{FL}}$ ($\omega_{\mathbf{FL}} \sim N(0, \mathbf{Q}_{\mathbf{FL}})$).

Finally, high frequency motions can be modeled by (Balchen *et al.*, 1980):

$$\dot{\mathbf{x}}_H = \begin{pmatrix} \mathbf{0}_{3x3} & \mathbf{I}_{3x3} \\ -\omega_0^2 \mathbf{I}_{3x3} & -2\zeta\omega_0 \mathbf{I}_{3x3} \end{pmatrix} \mathbf{x}_{\mathbf{L}} + \begin{pmatrix} \mathbf{0}_{3x3} \\ \mathbf{I}_{3x3} \end{pmatrix} \boldsymbol{\omega}_H \tag{5}$$

where $\mathbf{x}_H = \begin{pmatrix} \int X_H dt & \int Y_H dt & \int \psi_H dt & X_H & Y_H & \psi_H \end{pmatrix}^T$, $\boldsymbol{\omega}_H$ is a 3x1 vector containing zero-mean Gaussian white noises processes ($\boldsymbol{\omega}_H \sim N(0, \mathbf{Q}_H)$) and H represents high frequency. The parameter ζ is the relative damping ratio of the motions, and was set as 0.1. The parameter ω_0 should be the peak frequency of the motion power spectrum, which is close to the peak frequency of the wave spectrum, as explained in the previous section.

The measured signals **z** are given by:

$$\mathbf{z} = \begin{pmatrix} X_L + X_H + v_X \\ Y_L + Y_H + v_Y \\ \psi_L + \psi_H + v_\psi \end{pmatrix} \tag{6}$$

where **v** is a 3x1 vector containing zero-mean, Gaussian white noise processes ($\mathbf{v} \sim N(0, \mathbf{R})$).

Equations (3), (4), (5) and (6) were written as a discrete-time state space model and applied to a standard Kalman Filter. For the sake of simplicity, the matrixes $\mathbf{Q_L}$, $\mathbf{Q_H}$, $\mathbf{Q_{FL}}$ and $\mathbf{R}$ are considered diagonal in real applications.

It should be emphasized that the Kalman Filter estimates the components $\mathbf{x_H}$ and $\mathbf{x_L}$ and also low frequency environmental forces $\mathbf{F_E}$.

From now on, only one degree of freedom will be considered. Such simplification disregards the coupling between sway and yaw, presented in Eq. (1). Being *x* the controlled motion (surge, sway or yaw), and **x** the vector containing all Kalman filter model variables $\mathbf{x} = \begin{pmatrix} x_L, \dot{x}_L, \int x_H dt, x_H, F_E \end{pmatrix}^T$, the previous equations transform as:

$$\begin{aligned} \dot{\mathbf{x}} &= \mathbf{A}.\mathbf{x} + \mathbf{B}.\mathrm{F_T} + \mathbf{E}.\omega \\ \mathrm{z} &= \mathbf{H} \,.\, \mathbf{x} + \mathrm{v} \end{aligned} \tag{7}$$

$$\mathbf{A}=\begin{pmatrix} 0 & 1 & 0 & 0 & 0 \\ 0 & -c/m & 0 & 0 & 1/m \\ 0 & 0 & 0 & 1 & 0 \\ 0 & 0 & -\omega_0^2 & -2\zeta\omega_0 & 0 \\ 0 & 0 & 0 & 0 & 0 \end{pmatrix}; \mathbf{B}=\begin{pmatrix} 0 \\ 1/m \\ 0 \\ 0 \\ 0 \end{pmatrix}; \mathbf{E}=\begin{pmatrix} 0 & 0 & 0 \\ 1/m & 0 & 0 \\ 0 & 0 & 0 \\ 0 & 1 & 0 \\ 0 & 0 & 1 \end{pmatrix}; \mathbf{H}=\begin{pmatrix} 1 & 0 & 0 & 1 & 0 \end{pmatrix}; \omega=\begin{pmatrix} \omega_L \\ \omega_H \\ \omega_{FL} \end{pmatrix}$$

where *m* is the total mass related to the controlled motion (considering the added mass) and *c* is the damping term presented in matrix **C** of Eq. (3).

The following discrete version of Eq. (7) is used in the Kalman filter algorithm, being Δt the sampling time:

$$\begin{aligned} &\mathbf{x}[k] = \boldsymbol{\Phi}.\mathbf{x}[k-1] + \boldsymbol{\Delta}.F_T[k-1] + \boldsymbol{\Gamma}.\boldsymbol{\omega}[k-1] \\ &z[k] = \mathbf{H}.\mathbf{x}[k] + v[k] \\ &\boldsymbol{\Phi} = \mathbf{A}.\Delta t + \mathbf{I}; \boldsymbol{\Delta} = \mathbf{B}.\Delta t; \boldsymbol{\Gamma} = \mathbf{E}.\Delta t \end{aligned} \tag{9}$$

Being $\bar{\mathbf{x}}$ the *a priori* estimate and $\hat{\mathbf{x}}$ the *a posterior* estimate of state vetor, **X** the error matrix covariance and **K** the Kalman gain matrix, the discrete Kalman filter is given by (Cadet, 2003):

Prediction

$$\bar{\mathbf{x}}[k+1] = \mathbf{\Phi}.\hat{\mathbf{x}}[k] + \mathbf{\Delta}.F_T[k]$$
$$\bar{\mathbf{X}}[k+1] = \mathbf{\Phi}.\hat{\mathbf{X}}[k].\mathbf{\Phi}^T + \mathbf{\Gamma}.\mathbf{Q}.\mathbf{\Gamma}^T$$

Correction

$$\mathbf{K}[k] = \bar{\mathbf{X}}[k].\mathbf{H}^T.\left(\mathbf{H}.\bar{\mathbf{X}}[k].\mathbf{H}^T + \mathbf{R}\right)^{-1}$$
$$\hat{\mathbf{x}}[k] = \bar{\mathbf{x}}[k] + \mathbf{K}[k].\left(z[k] - \mathbf{H}.\bar{\mathbf{x}}[k]\right) \quad \text{with } \mathbf{Q}_{3x3} = \begin{pmatrix} Q_L & 0 & 0 \\ 0 & Q_H & 0 \\ 0 & 0 & Q_{FL} \end{pmatrix}$$
$$\hat{\mathbf{X}}[k] = \left(I - \mathbf{K}[k].\mathbf{H}\right).\bar{\mathbf{X}}[k] \tag{10}$$

The frequency ω_0 must be estimated, since it plays an important role in the filter performance. Commercial DPS contains algorithms to perform such on-line estimation, but the complete mathematical formulation is not described by the manufacturers. Ljung (1987) presents several methods that can be applied in this problem, and in the present work the Recursive Prediction Error Method was adopted. The same method was used in the seminal work of Balchen et al. (1976).

Being the innovation $\varepsilon[k] = z[k] - \mathbf{H}.\bar{\mathbf{x}}[k]$ and $\hat{\omega}_0[k]$ the frequency estimate at a sample time *k*, the RPE equations are given by:

$$\hat{\omega}_0[k] = \hat{\omega}_0[k-1] + \frac{P[k-1]\psi[k]}{\lambda + P[k-1]\psi[k]^2}\varepsilon[k]$$
$$P[k] = \frac{1}{\lambda}\left[P[k-1] - \frac{P[k-1]^2\psi[k]^2}{\lambda + P[k-1]\psi[k]^2}\right] \tag{11}$$

where λ is the forgetting factor (taken as 0.996 in the present work), $\psi[k] = -\partial\varepsilon/\partial\hat{\omega}_0$, $P[k]$ is an estimate of cov($\psi[k]$). The sensitivity function $\psi[k]$ can be evaluated by:

$$\psi[k] = -\frac{\partial\varepsilon}{\partial\hat{\omega}_0} = -\frac{\partial(z[k] - \mathbf{H}.\bar{\mathbf{x}}[k])}{\partial\hat{\omega}_0} \cong \mathbf{H}\frac{\partial\bar{\mathbf{x}}[k]}{\partial\hat{\omega}_0} \tag{12}$$

Using Eq.(10), one can show that $\bar{\mathbf{x}}[k+1] = \hat{\mathbf{\Phi}}.\bar{\mathbf{x}}[k] + \mathbf{\Delta}.F_T[k] + \hat{\mathbf{\Phi}}.\mathbf{K}[k].\varepsilon[k]$, being $\hat{\mathbf{\Phi}} = \mathbf{\Phi}(\hat{\omega}_o)$, leading to:

$$\frac{\partial\bar{\mathbf{x}}[k+1]}{\partial\hat{\omega}_0} = \hat{\mathbf{\Phi}}.\frac{\partial\bar{\mathbf{x}}[k]}{\partial\hat{\omega}_0} + \hat{\mathbf{\Phi}}.\mathbf{K}[k].\frac{\partial\varepsilon[k]}{\partial\hat{\omega}_0} + \frac{\partial\hat{\mathbf{\Phi}}}{\partial\hat{\omega}_0}.\left(\bar{\mathbf{x}}[k] + \mathbf{K}[k].\varepsilon[k]\right) + \hat{\mathbf{\Phi}}.\frac{\partial\mathbf{K}[k]}{\partial\hat{\omega}_0}.\varepsilon[k] \tag{13}$$

disregarding the dependency of **K**[k] on $\hat{\omega}_0[k]$, Eq. (13) and (12) lead to the following algorithm to evaluate the sensitivity function:

$$\frac{\partial\bar{\mathbf{x}}[k+1]}{\partial\hat{\omega}_0} = \hat{\mathbf{\Phi}}.\left[I - \mathbf{K}[k].\mathbf{H}\right].\frac{\partial\bar{\mathbf{x}}[k]}{\partial\hat{\omega}_0} + \frac{\partial\hat{\mathbf{\Phi}}}{\partial\hat{\omega}_0}.\hat{\mathbf{x}}[k]$$
$$\psi[k+1] = \mathbf{H}\frac{\partial\bar{\mathbf{x}}[k+1]}{\partial\hat{\omega}_0} \tag{14}$$

Figure 4 presents a block diagram of the Kalman filter and the controller, which will be analyzed in the next section. It must be noticed that DP systems normally contain a feed forward loop to compensate wind effects. Wind speed and direction are measured by anemometers, and the forces are evaluated using the wind coefficients of the ship. Such forces are directly compensated by the controller, and they are counteracted before causing a positioning error. These estimates are also used by the Kalman filter, which must subtract them from the total thrust forces, resulting the parcel of thrust responsible for current and wave compensation. In the present work, such feed forward loop is not considered.

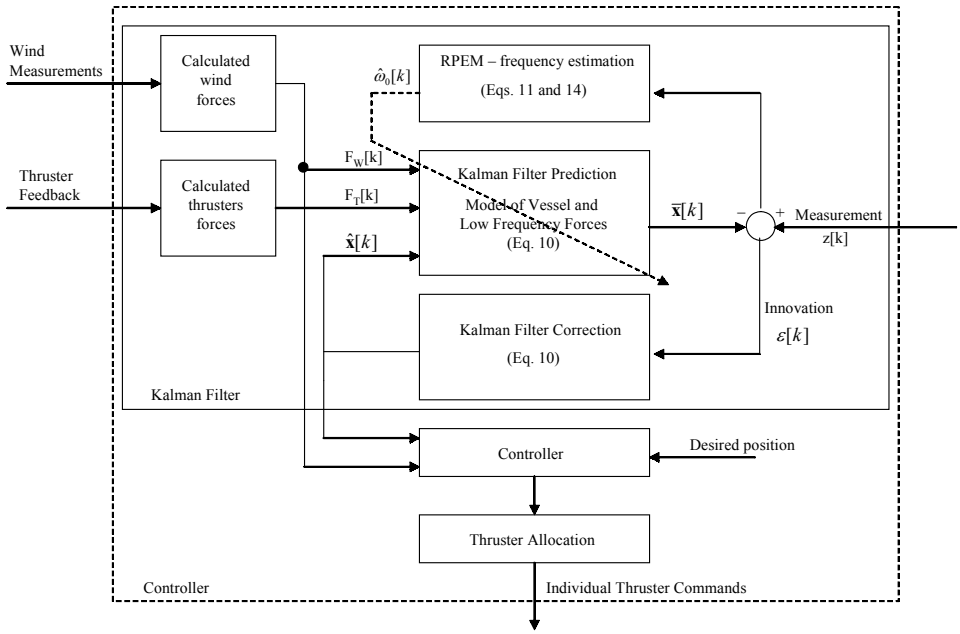

Figure 4. Kalman filter and controller block diagram

4. Model reference adaptive controller design

The idea behind the so-called model-reference adaptive control is to design a controller whose action on the plant under study is such that its response tracks that of a pre-established dynamic system, which is otherwise known as the reference model. Hence the name *model-reference adaptive control* (MRAC for short). The dynamic behavior of the reference model is represented by Eq. (15) and the plant dynamics is given in Eq.(16). A complete derivation of the MRAC can be found in Slotine and Li (1991).

$$M_m \ddot{y}_m + B_m \dot{y}_m + K_m y_m = u_c(t) \tag{15}$$

$$M\ \ddot{y} + B\ \dot{y} = u(t) \tag{16}$$

Note that for the present offshore operation, K=0, which basically means that the vessel is deprived of any sort of moorings. We shall now introduce z(t):

$$z(t) = \ddot{y}_m - \beta_1 \dot{e} - \beta_0 e \tag{17}$$

where $e = y - y_m$. It follows from this definition that e is expected to converge asymptotically to zero (the plant matches the reference model). Now, let us define the vector $\mathbf{v} = [z(t)\ \ \dot{y}\ ]^T$ and the vector of estimated parameters $\hat{\mathbf{a}}(\mathbf{t}) = [\hat{a}_2\ \hat{a}_1\ ]^T$. In doing so, we have laid the basis to define the control law, which is given by:

$$u(t) = \hat{a}_2 z(t) + \hat{a}_1 \dot{y} \tag{18}$$

At this point, all that is left is to evaluate the law for the adaptation mechanism. The error ($e = y - y_m$) dynamics can be written as:

$$\ddot{e} + \beta_1 \dot{e} + \beta_0 e = (1/a_2)\, \mathbf{v}^{\mathbf{T}}(\mathrm{t}).\tilde{\mathbf{a}}(\mathrm{t}) \tag{19}$$

where β_0 and β_1 are positive constants such that $s^2 + \beta_1 s + \beta_0$ is a stable (Hurwitz) polynomial. And $\tilde{\mathbf{a}}(\mathrm{t})=\hat{\mathbf{a}}(\mathrm{t})-\mathbf{a}(\mathrm{t})$. Equation (19) can be rewritten in the state-space form as:

$$\dot{\mathbf{x}} = \mathbf{A}\mathbf{x} + \mathbf{b}[(1/a_2)\mathbf{v}^{\mathbf{T}}\tilde{\mathbf{a}}] \quad \text{with } \mathbf{A} = \begin{pmatrix} 0 & 1 \\ -\beta_0 & -\beta_1 \end{pmatrix};\ \mathbf{b} = \begin{pmatrix} 0 \\ 1 \end{pmatrix};\ \mathbf{x} = \begin{pmatrix} e \\ \dot{e} \end{pmatrix} \tag{20}$$

Introducing the matrices $\boldsymbol{\Gamma}$, $\mathbf{P}$ and $\mathbf{Q_C}$, being $\boldsymbol{\Gamma}$ and $\mathbf{P}$ symmetric positive definite constant matrices, $\mathbf{PA} + \mathbf{A}^{\mathbf{T}}\mathbf{P} = -\mathbf{Q}_{\mathrm{C}}$, $\mathbf{Q}_{\mathrm{C}} = \mathbf{Q}_{\mathrm{C}}^{\ \mathrm{T}} > 0$, for a chosen $\mathbf{Q_C}$. The adaptation law is then given by:

$$\left(\dot{\hat{a}}_2 \quad \dot{\hat{a}}_1\right)^T = -\boldsymbol{\Gamma}.\mathbf{v}.\mathbf{b}^T.\mathbf{P}.\mathbf{x} \tag{21}$$

A block diagram of the controller is presented in Fig. 6.

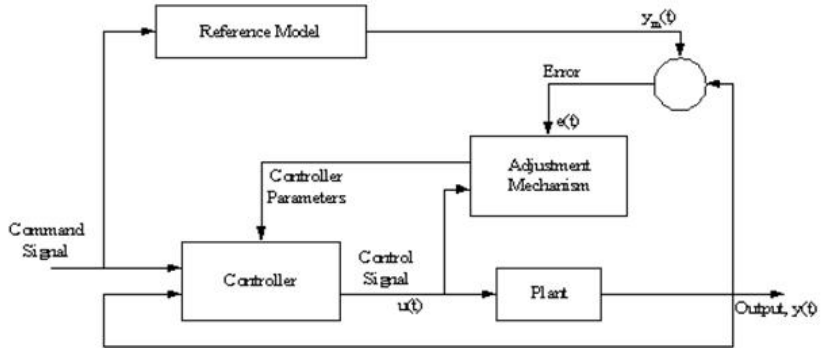

Figure 6. Model reference adaptive controller

Convergence properties can be proved using the following Lyapunov function and its time derivative:

$$\mathbf{V(x,\tilde{a})} = \mathbf{x}^T\mathbf{P}\mathbf{x} + \tilde{\mathbf{a}}^T\boldsymbol{\Gamma}^{-1}\tilde{\mathbf{a}} \tag{22}$$
$$\dot{\mathbf{V}} = -\mathbf{x}^T\mathbf{Q}_C\,\mathbf{x} + 2\tilde{\mathbf{a}}^T\mathbf{v}\mathbf{b}^T\mathbf{P}\mathbf{x} + 2\tilde{\mathbf{a}}^T\boldsymbol{\Gamma}^{-1}\dot{\tilde{\mathbf{a}}} = -\mathbf{x}^T\mathbf{Q}_C\,\mathbf{x}$$

It is possible to show the convergence of **x** using Barbalat´s lemma. Therefore with the adaptive controller defined by both the adaptation and the control law, **x** converges to zero. The condition for parameter convergence can be shown to be the *persistent excitation* of the vector **v**.

Using $\beta_0 = K_m/M_m$ and $\beta_1 = B_m/M_m$, the polynomial $s^2 + \beta_1 s + \beta_0$ will be obviously stable. Substituting Eq.(18) in Eq.(16), one obtains the following closed loop dynamics:

$$M\,\ddot{y} + B\,\dot{y} = \hat{a}_2 z(t) + \hat{a}_1\dot{y} \tag{23}$$

Using Eq. (17) and (15), Eq.(23) can be written as:

$$M\,\ddot{y} + B\dot{y} = \hat{a}_2\left(\frac{u_c(t)}{M_m} - \beta_1\dot{y} - \beta_0 y\right) + \hat{a}_1\dot{y}$$
$$\frac{M.M_m}{\hat{a}_2}\ddot{y} + \frac{.M_m}{\hat{a}_2}\left(B + \hat{a}_2\beta_1 - \hat{a}_1\right)\dot{y} + \hat{a}_2\beta_0 y = u_c(t) \tag{24}$$

Since the tracking error converge to zero, Eq.(24) converges to the reference model Eq.(15), what is only possible if $\hat{a}_2 \to M$ and $\hat{a}_1 \to B$.

The analogy between a PD controller and the previously derived MRAC is obtained by means of Eq. (18), that can also be written as:

$$u(t) = -\hat{a}_2\beta_1\dot{e} + \hat{a}_1\dot{y} - \hat{a}_2\beta_0 e + \hat{a}_2\ddot{y}_m$$

where the first and second terms are responsible for the derivative action and the third term gives the proportional action. For the surge motion, in which the damping factor B is extremely small ($B \ll B_m$), the equivalent constant *P* and *D* gains are given by:

$$P = -\hat{a}_2\beta_0 = -M.\frac{K_M}{M_M} \qquad ; \qquad D = -\hat{a}_2\beta_1 = -M.\frac{B_M}{M_M} \tag{25}$$

5. Case study

The controller was implemented in a numerical simulator, considering a real shuttle vessel operating in Brazilian waters during an offloading operation (Fig. 6). The main properties of the tanker in both, ballasted and loaded, conditions are presented in Table 1.

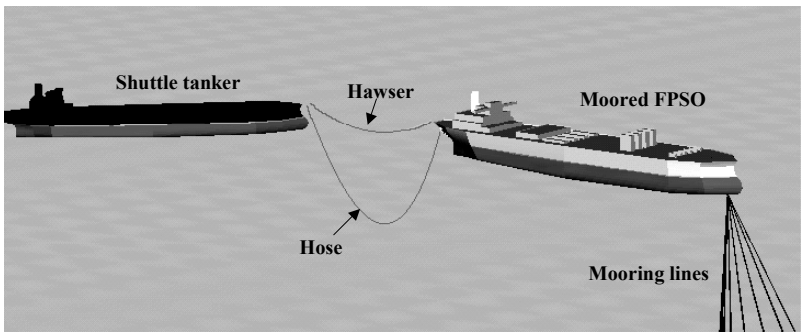

Figure 6. (Left) Offloading operation; (Right) Picture of shuttle tanker in ballasted condition

Table 1. Tanker main properties.

Property	**Full load condition**	**Ballasted condition**
Length (L)	260 m	
Beam (B)	44.5 m	
Draft (T)	16.1 m	6. 4 m
Mass (M)	156,310 ton	58,783 ton
Surge Added Mass (M_{11})*	1,560 ton	8,510 ton

* **Low frequency**

A 12h offloading operation was simulated, in which the tanks of the ballasted ship are fulfilled with the oil transferred from the FPSO. The shuttle tanker is kept aligned with the FPSO, in a distance of approximately 100m. Therefore, surge motion control is critical, due to the risk of collision or else rupture of the hose. So, FPSO position must be monitored and, in case of large amplitude motions, DPS must relocate the shuttle to keep a safe distance. In order to analyze controller performance, it was considered corrections of 20m each 30min. This simulation tries to recover the real control approach used in DPS installed in shuttle vessels. In order to save fuel, the shuttle tanker does not follow all motions of FPSO, being only relocated when the FPSO presents a large displacement (Bravin and Tannuri, 2004). Figure 7 shows the environmental condition and the set-point considered in the simulations.

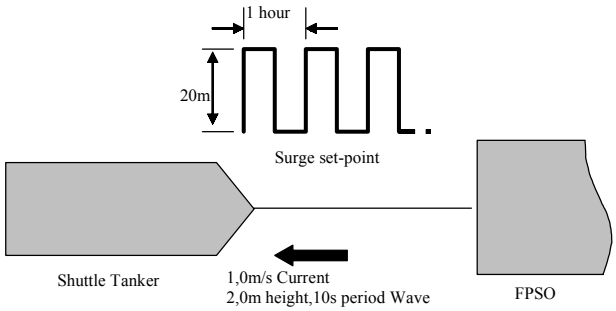

Figure 7. Set-point and environmental conditions

Main control and filter parameters are given by:

$$\mathbf{Q}_{3x3} = \begin{pmatrix} 4\times10^{10} & 0 & 0 \\ 0 & 2.6 & 0 \\ 0 & 0 & 1.2\times10^{10} \end{pmatrix} ; \mathrm{R} = 1 ; \mathbf{\Gamma}_{2x1} = \begin{pmatrix} 4\times10^{10} & 0 \\ 0 & 8\times10^{6} \end{pmatrix} ; Q_{C\,2x1} = \begin{pmatrix} 1 & 0 \\ 0 & 1 \end{pmatrix} \times 6.5\times10^{-6}$$

Figure 8 shows the simulation result considering the adaptive control. The reference model is a second order system with a natural period of 200s and damping factor of 1.0 (no overshoot). The reference model is tracked with good accuracy by the ship, despite the mass variation, with no performance loss. After a short transient, the tracking error $e = y\text{-}y_m$ is reduced to values smaller than 0.5m, being mainly represented by the non-controlled high-frequency motions. Figure 9 presents control force, which gets higher during the simulation, due to the increasing of mass, damping, wave and current forces.

The adaptive controller estimation of the components of vector **â(t)** (mass and damping, as already explained), are shown in Fig. 10. The mass estimation presents very good accuracy and an oscillatory behavior was found in damping estimation. This fact was expected, since damping effect in surge motion is extremely small, what is confirmed by the very good performance of the system (Fig. 8) despite such estimation error. Figure 11 confirms that Kalman filter high frequency motion estimation works properly. The estimation of the surge motion peak period converges to 12,5s, recovering the value theoretically evaluated by Eq.(2). As already mentioned, this value is close to the peak period of waves (10s in the present case).

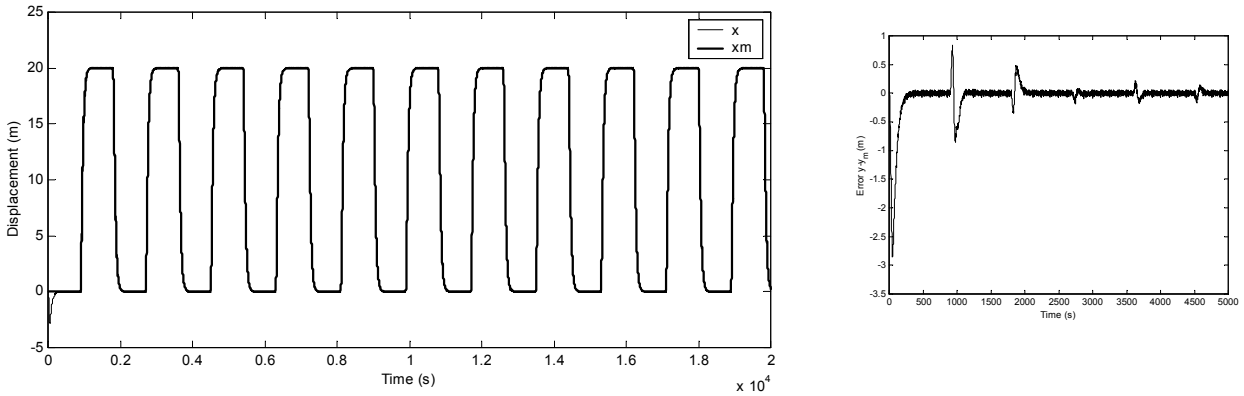

Figure 8. (Left) Surge position and reference model output (Right) Tracking error $e = y - y_m$

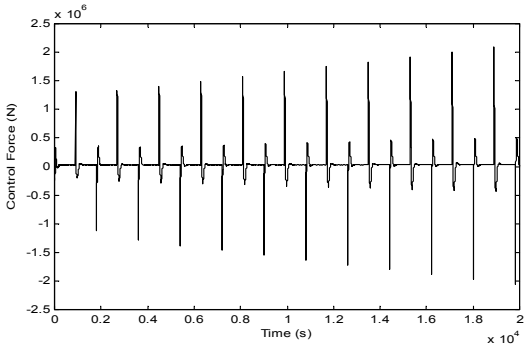

Figure 9. Control force

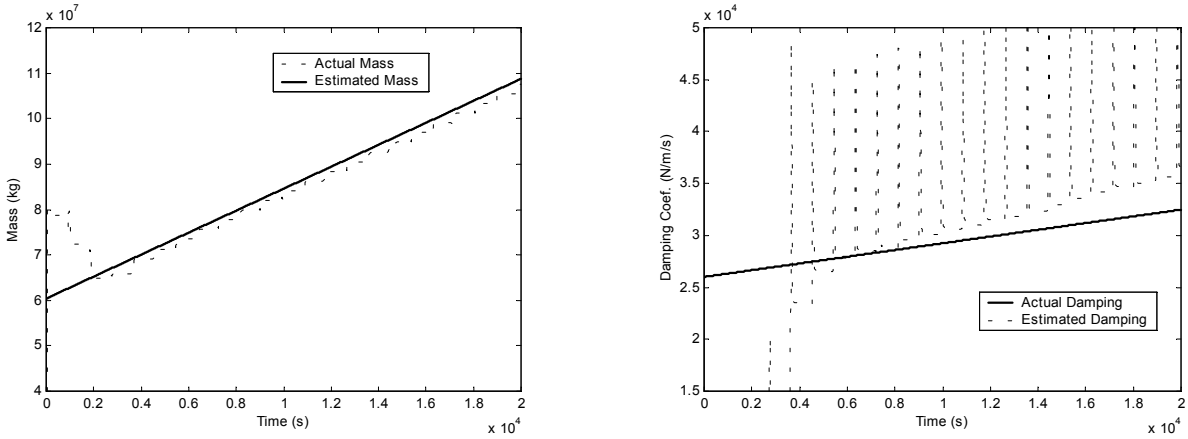

Figure 10. Parameter estimation. (Left) Mass ; (Right) Damping

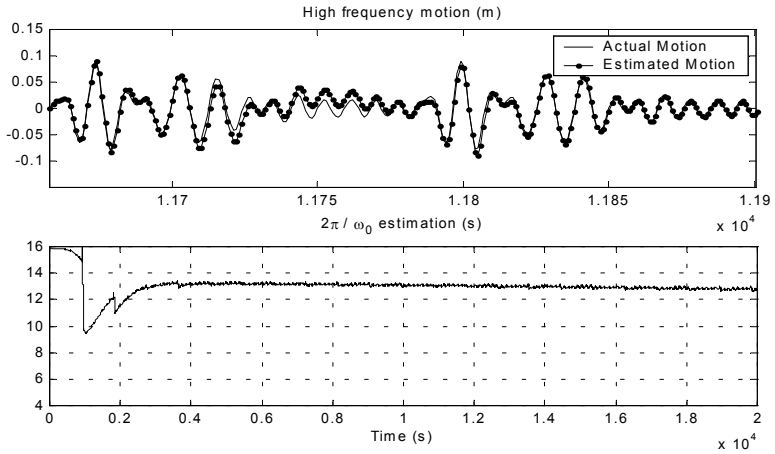

Figure 11. (Up) Kalman filtering high frequency motion estimation ; (Down) ω_0 estimation by RPEM

The PD controller with constant gains was also applied to the problem, and the simulation result is presented in Fig. 12. It becomes evident the performance loss during the offloading operation, as the mass and dynamic properties of the

ship changes. Since the P and D parameters of the controller was evaluated by Eq. (25) considering the ballasted mass of the ship, the performance of the controller is better in the beginning of the operation, getting worse as the inertia increases. The overshoot of closed loop response increases, what may cause dangerous approximations of the ships.

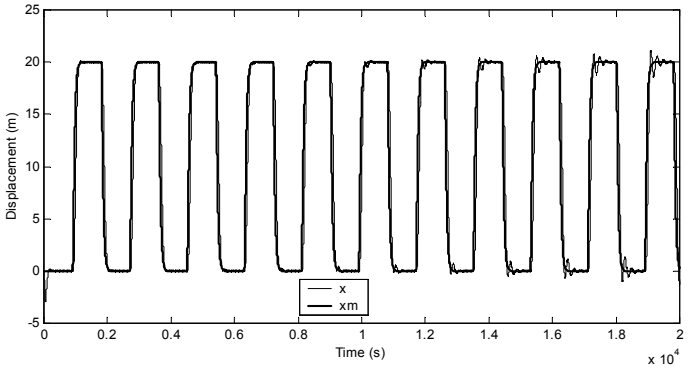

Figure 12. Actual position and set-point

6. Conclusions

This work presented the application of model-based adaptive control techniques to DPS's, cascaded with the commonly used adaptive Kalman filter. The controller was applied to a dynamic positioned shuttle tanker subjected to waves and current, during the offloading operation. The results showed that a good performance is kept during all the operation, despite the significant variations in dynamic properties of the vessel due to oil transfer. The adaptive algorithm was able to estimate the mass of the vessel with a good accuracy and to adjust the controller. For the sake of comparison, a PD controller with constant gains was also applied, and it was showed that such controller is not able to cope with variations in dynamic properties of the vessel, and a loss in performance was observed during the operation.

7. Acknowledgements

This work has been supported by Petrobras and the State of São Paulo Research Foundation (FAPESP – Process no. 03/12330-3). A CNPq research grant, process no.302450/2002-5, is also acknowledged.

8. References

Aarset, M.F., Strand, J.P. and Fossen, T.I., 1998, "Nonlinear Vectorial Observer Backstepping With Integral Action and Wave Filtering for Ships", Proceedings of the IFAC Conference on Control Applications in Marine Systems (CAMS'98), Fukuoka, Japan, pp.83-89.

Balchen, J.G., Jenssen, N.A. and Saelid, S., 1976, "Dynamic Positioning using Kalman Filtering and Optimal Control Theory", Proceedings of IFAC/IFIP Symposium on Automation in Offshore Oil Field Operation, Bergen.

Balchen, J.G. et al., 1980, "A dynamic positioning system based on Kalman filtering and optimal control", Modeling, Identification and Control, Vol. 1, No. 3, pp. 135-163.

Bravin, T.T. and Tannuri, E.A., 2004, "Dynamic Positioning Systems Applied to Offloading Operations", International Journal of Maritime Engineering (IJME), to appear.

Bray, D., 1998, Dynamic Positioning, The Oilfield Seamanship Series, Volume 9, Oilfield Publications Ltd. (OPL).

Cadet, O., 2003, "Introduction to Kalman Filter and its use in Dynamic Positioning Systems", Proceedings of Dynamic Positioning Conference, September 16-17, Houston, USA.

Fossen, T.I., 1994, "Guidance and Control of Ocean Vehicles", John Wiley & Sons, 479p.

Katebi, M.R., Grimble, M.J. and Zhang, Y. (1997), "H_∞ robust control design for dynamic ship positioning", IEE Proc. Control Theory Appl, Vol.144, No.2, pp. 110-120.

Kongsberg Simrad, 1999, "Operator Manual Kongsberg Simrad SDP (OS)", Rel 2.5, Norway, 412 p.

Ljung, L., 1987, System Identification, Theory for the User, Prentice Hall, Inc., Englewood Cliffs, New Jersey.

Saelid, S., Jenssen, N.A. and Balchen, J.G., 1983, "Design and Analysis of a Dynamic Positioning System Based on Kalman Filtering and Optimal Control", IEEE Transactions on Automatic Control, Vol.AC-28, No.3, pp. 331-339.

Slotine, J.J.E.; Li, W. , 1991, "Applied Nonlinear Control", Prentice Hall, New Jersey.

Tannuri, E.A., Donha, D.C. and Pesce, C.P., 2001, "Dynamic Positioning of a Turret Moored FPSO Using Sliding Mode Control", International Journal of Robust and Nonlinear Control, Vol.11, pp.1239-1256, May.

Tannuri, E.A., Bravin, T.T. and Pesce, C.P., 2003, "Dynamic Positioning Systems: Comparison Between Wave Filtering Algorithms and Their Influence on Performance", Proceedings of 22nd International Conference on Offshore Mechanics and Arctic Engineering (OMAE2003 Conference), June 3-13, Cancun, Mexico.

9. Responsibility notice

The authors are the only responsible for the printed material included in this paper.